

Development of a Porcine FE Model for the Investigation of Spondylolytic Vertebral Fractures

Colin Bright, Stephen Tiernan, Fiona McEvoy

Institute of Technology, Tallaght

Tallaght, Dublin 24, Ireland

colinbright@ittd.ie; stephen.tiernan@ittdublin.ie; fiona.mcevoy@ittdublin.ie

Pat Kiely

Our Lady's Children's Hospital

Crumlin, Dublin, Ireland

Abstract - As many as 85% of adults experience back pain that interferes with their work and leisure activities, and 25% of people between the ages of 30–50 years report lower back pain symptoms. In normal healthy bone, very small cracks form and heal on an on-going basis, these small cracks help the bone adapt to the loads it has to carry by directing bone repair and remodelling. When this repair process cannot keep up with the propagation and coalescence of cracks, a fracture can occur. The occurrence of such fractures in the lower lumbar segments of the spinal column of young athletes is a well-documented problem, and is given the clinical name spondylolysis.

Fracture events in bone are known to be strain controlled. The purpose of this work is to statically validate a finite element model of a porcine vertebra. This FE model of the porcine L4 vertebra was developed from CT scans, material properties were applied on a per-voxel basis using published empirical formulae. This model was used to estimate the stiffness in response to static loads. A complementary experimental study was completed using static compression tests on both porcine vertebral bodies and full vertebrae. Results for full vertebrae showed agreement between the measured average stiffness (578 N/mm, SD 10.4) and the stiffness of the FE model (553 N/mm).

Keywords: Spine, Fracture, Spondylolysis, FEA.

1. Background

A large proportion of adults experience back pain that interferes with their work and leisure activities. Much of the pain and discomfort in later life has resulted from an untreated condition during adolescence. Vertebral stress fractures in otherwise healthy, athletic adolescents are a well-documented problem (HensingerRN, 1989)(Wiltse, 1957). The neural arch of the vertebra, specifically the portion between the articular facets, known as the pars interarticularis, is particularly susceptible. Stress fractures in this region are given the clinical name spondylolysis. While a considerable volume of work exists on the links between athletic technique and spondylolysis (Crewe, 2013), the link between magnitude and frequency of the applied load and resulting pars interarticularis fracture remains unknown. This will be elucidated through the development of a validated FE model and this forms the novel element of this research.

1.1 Porcine Spinal Specimens

The study of human spinal conditions presents a number of challenges, such as the availability of suitable specimens from the young population. Many researchers therefore use animal models, with advantages being the homogeneity of specimen, plentiful supply and the avoidance of harmful pathogens associated with un-embalmed human cadavers (Dickey, 2003)(Lin, 1997)(Kettler, 2007). Popular alternatives to human specimens are porcine, ovine, bovine (Taylor et al., 2010) and porcine (Schmidt, 2005). Teoh & Chui (2008), referring to the work of Smit (2002) reports that *“There are no substantial experimental or theoretical studies proving that quadrupeds (e.g. pigs) are subjected to loads different*

from biped spines (e.g. humans)”. A porcine model was chosen for this study based on availability and the close biomechanical match to human (Dath, 2007),(Busscher et al., 2010)&(Wilke, 2011). The choice of porcine spine region to give the closest approximation is important. The region of porcine spine that gives the best kinematic approximation to the human lumbar spine is the porcine lower cervical and upper thoracic spine, from C5 – T1. This region exhibits a close biomechanical match with the lower human lumbar spine in terms of range of motion and as reported by Kuo & Wang (2007) the closest match of facet joint angle. However, as this study is focussing on fracture of a single vertebra, where kinematics is not considered, it is hypothesised that bone volume is the dominant criteria for selection. For that reason the lower lumbar porcine vertebrae were chosen (L3 – L5). Human lumbar vertebrae are the largest in the spinal column, with the 5th lumbar vertebra known to be the stiffest (Teoh & Chui, 2008).

The porcine spine as a model for human has received attention in a number of biomechanical studies. Howarth et al., (2011 & 2013) in a study of cumulative loading of the porcine cervical-thoracic spine discovered that the maximum level to level shear forces are approximately 2kN. Howarth also reported a non-linear relationship between joint shear load and fatigue life. (Bisschop et al., 2012) in a study of joint shear force before and after laminectomy reported an average reduction in shear force to failure of 845N when the lamina of the vertebra is removed. Wilcox (2007) in a study of vertebral body uniaxial stiffness carried out tests on porcine L3 vertebrae, specimen stiffness ranged from 3.30 to 6.03 kN/mm (mean = 4.62 kN/mm) and the strength from 6.83 to 11.79 kN (mean = 9.14 kN).

An important consideration when examining cracking and fracture in porcine bone is the underlying microstructure. Tanck et al., (2001) examined the hypothesis that increase in bone volume fraction precedes architectural adaptation in porcine bone. Porcine tibia and vertebrae were examined using μ CT at ages of 6, 23, 56, 104 and 230 weeks. It was discovered that with the rapid increase in weight in early life, bone density also increases and that morphological anisotropy only begins to increase after 23 weeks. Morphological anisotropy continues to increase until 104 weeks before stabilising. Tanck and co-workers also reported that elastic modulus increased with age until 104 weeks, with an average modulus of 700MPa at 23 weeks. This increase in elastic modulus was attributed to bone volume fraction in the period between 6 weeks and 56 weeks, thereafter it was attributed to the change in degree of anisotropy.

The work of Tanck and co-workers suggests that the choice of specimen age should be based on the clinical condition being examined. In the case of this work on spondylolysis, an immature animal is preferred as the bone more closely matches that of an adolescent human.

1.2 Finite Element Model

The use of finite element models for the study of biomechanics is well established (Huiskes, 1983),(Prendergast, 1997). The principal challenges faced are the accurate representation of both geometry and material properties. The key to building the most efficient model possible is the simplifications that are made, Prendergast & Lennon (2007) state that *‘Appropriate simplifications depend on the hypothesis about the behaviour of the system you want to test with the model’*. In this case it is the stiffness and fracture resistance of the vertebral neural arch. To that end the method of generating an FE mesh from computed tomography scans and the subsequent application of material properties on a “per-voxel” basis are reviewed below.

Computed tomography scanning exposes bone segments to x-rays, these x-rays are detected after they have passed through the bone material, the detected signal is related to a grey value and that grey value is related to a standardised CT measurement unit called the Hounsfield unit.

Teo et al.,(2006) in a study of porcine bone discovered that trabecular bone has a Hounsfield range of 219.35 – 738.11 HU, compared to human with a range 112 – 258 HU (Hobatho et al, 1997). Rho (Rho et al., 1995) in a study of the relationship between Hounsfield unit derived material properties and experimentally derived properties, discovered that compressive mechanical properties correlate well to density from Hounsfield units, however as stated by Teo et al., (2006) bone mineral density alone is not a good predictor of the likelihood of osteoporotic fracture, what is also required is a measure of the orientation and level of interconnectedness of the bone to expand the viability of this technique beyond uniaxial testing. In fact many authors agree that 30-50% of unaccounted variance still exists in

mechanical properties when applied using this method (Keaveny & Yeh, 2002)(Van Lenthe, Van Den Bergh, Hermus, & Huiskes, 2001). In order to quantify the validity of using this method Teo et al., (2006) investigated how well bone morphology can be predicted and at which resolution CT scanning should be carried out in order to do this. Teo and co-workers carried out a micro CT study which was evaluated using quantification factors for trabecular bone which were developed by Parfitt, (1987). These calculated bone quality factors were compared with physical testing and it was found that at their resolution level (14.836µm) a moderate correlation was shown between Hounsfield units and Trabecular Bone Pattern Factor (Tb.Pf) and Structure Model Index (SMI) with R² values of 0.796 and 0.709 respectively. Later studies by Muller & Ruegsegger, (1997) and Cendre et al., (1999) discovered that the ability to calculate these numbers was based on a minimum resolution of 100µm.

Many of the authors mentioned above used their experimental data to create empirical formulae based on Hounsfield or grey value conversion. Carter and Hayes propose the following formulae based on their micro CT study of human trabecular bone:

Density:

$$\rho = 47 + 1.122\text{HU} \text{ [kg/cm}^2\text{]} \quad (1)$$

And elastic modulus:

$$E = 3790\varepsilon^{0.06}\rho^3 \text{ [MPa]} \quad (2)$$

Table 1. Glossary of terms for equation 1 & 2.

ρ	Density
E	Young's Modulus
ε	Strain Rate
HU	Hounsfield Unit

Note: Empirical relationship for strain rate was based on uniaxial compression tests.

2 Materials and Methods

2.1 Stiffness of Pars Interarticularis

Six lower lumbar vertebrae, L4 & L5 from 2 different pigs (6 months old, average 71 kg) were dissected of all soft tissue and manually cleaned so that the bone surface was not damaged. The vertebrae were mounted in polyurethane so that the superior end plate and superior facets were constrained.

A jig was manufactured to hold the vertebrae so that the inferior facet surface was loaded normal to its articulating surface. The adjacent facets (cranial to caudal) in the porcine spinal column form a partial cup and cone structure (**Error! Reference source not found.**) with the inferior facets bi-laterally constrained, this has led to a developmental optimisation (bone modelling) of the bone material between the inferior facets. This observation led to an enhancement in test method, whereby the inferior facets were mounted in polyurethane preventing lateral displacement, representing the physiological situation.

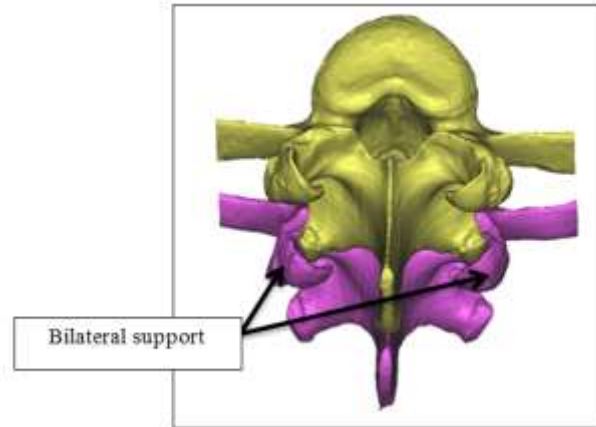


Fig.1. Posterior view of porcine spine showing "cup and cone" arrangement of facets.

The jig was mounted in an Instron Series 3345 (3kN) test machine, the machine was set to run to a maximum load of 2kN at a rate of 5mm/s (B.M. Cyron, W.C. Hutton, 1976).

2.2 Stiffness of Vertebral Body

The test protocol employed here follows the methods of Singer, (1995) who carried out compression tests on human thoracic and lumbar vertebral bodies. Testing was carried out using the MTS Bionix Servo hydraulic Test System.

Singer process was as follows:

- Pre-load 250N and hold for 60s
- Load to zero
- Compress at 0.25mm/s to failure
- Failure is classified as 10% reduction in height

Two further porcine vertebrae were dissected of all soft tissue; the posterior portions of the vertebra were removed. The specimens were mounted in polyurethane at their cranial and caudal extremes (**Error! Reference source not found.**). Specimens were stored in a fridge at 3°C prior to testing; they were wrapped in tissue and soaked with saline to prevent further dehydration.



Fig. 2. Specimen for uniaxial compression testing of porcine vertebra body.

2.3 Finite Element Model

A finite element model of the 4th lumbar vertebra was created. CT scans were analysed and a tetrahedral mesh was generated using Mimics medical imaging software (Materialise NV, Belgium). Material properties were applied using the CT grey values which were converted to Hounsfield units (HU); these were then used to calculate density (ρ) and Young's modulus (E) using equation (1) and (2). This model was used for the evaluation of stiffness of pars interarticularis (Test Group 1). However, in

order to match the test conditions for the vertebral body compression tests (Test Group 2), the posterior elements of the vertebra must be suppressed, and as this model was built from CT data, not CAD geometry, a novel method was employed to identify the elements concerned and achieve the suppression.

- Using Ansys Mechanical workbench the nodes relating to the “unwanted” posterior portions were identified.
- An Ansys Classic input file was written in workbench, this file was opened in Ansys Classic and an attribute list was generated giving elements and associated nodes.
- Microsoft Excel was used to cross reference the list of unwanted nodes against the full list of nodes and their associated elements, thus generating a list of unwanted elements, those of the posterior portions of the vertebra.
- The materials for this model were applied using a command code generated by Materialise Mimics. That code was edited to include a new material with a stiffness = 1Pa.
- The material allocation code was then rewritten, assigning the new material to 37000 elements that make up the unwanted section.
- When this code is implemented the posterior portions of the model make no significant contribution to stiffness (**Error! Reference source not found.**).

3 Results

3.1 Stiffness of Pars Interarticularis

The average results for pars interarticularis stiffness were 578 N/mm, SD 10.4. As a model for human lumbar vertebrae the experimental values compare moderately well with those of Cyron & Hutton (1976) who reported average stiffness values of 492 N/mm for human L5 vertebrae. The FE model as described in section 2.3 shows very good agreement with the experimental results with a stiffness value of 553 N/mm.

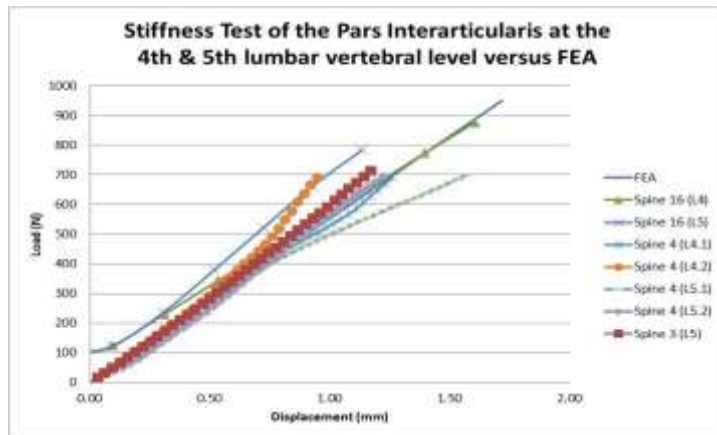


Fig. 3. Test results for vertebral stiffness and FEA.

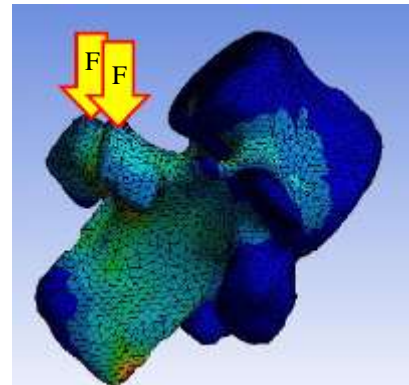


Fig. 4. FE Model.

3.2 Stiffness of Vertebral Body

The results for the vertebral body compression tests yielded values of 4.28 kN/mm, at the L3 level, and 6.02 kN/mm, at the L4 level. The FE model, of the L4 vertebra had a stiffness of 5.75kN/mm which is in good agreement with the experimental values with a difference of <5%. The L3 experimental results are in good agreement with values, 4.62 kN/mm, published by Wilcox (2007) for porcine L3 vertebra.

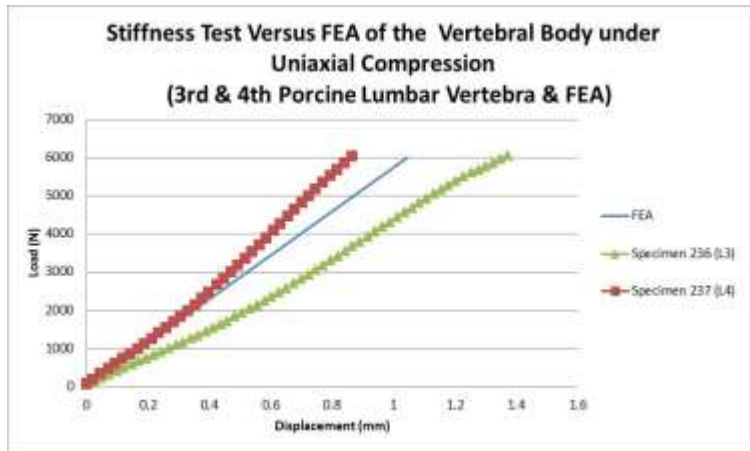


Fig. 5. Vertebral Body Compression results.

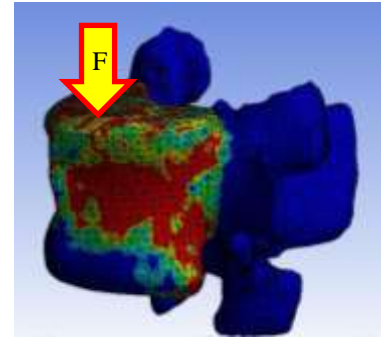


Fig. 6. VonMises stress plot for vertebral body.

4. Discussion

An FE model of the porcine 4th lumbar vertebra has been presented. This model has been validated using 2 different tests. This validated FE model is a good predictor of vertebral stiffness and provides an accurate computational model for the evaluation of spondylolytic fractures. It's important to note that the clinical condition under investigation is a fatigue fracture, not a fracture resulting from overload. Fatigue fractures in bone are known to be strain controlled in initiation (Nalla et al., 2005). A pilot study was undertaken to measure the strains in pars interarticularis of the porcine L4 vertebra and evaluate the potential of the FE model in reproducing those strains.

Two porcine L4 vertebrae were prepared for testing as described in section 2.1. The posterior pars interarticularis was cleaned of all soft tissue using a scalpel and grade 400 sand paper, the bone was then degreased using Vishay GC-6 isopropyl alcohol. A Vishay EA-06-060RZ-120 rectangular rosette strain gauge was fitted using M-Bond AE10 (2 part resin). The specimen was mounted on the jig described in section 2.1 which was in turn mounted in an MTS Bionix Servo hydraulic Test System (**Error! Reference source not found.**).

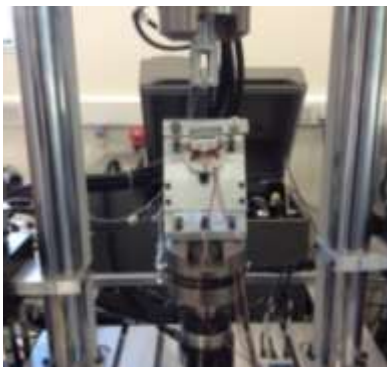


Fig. 7. Test setup MTS Bionix.



Fig. 8. Wired up gauge.



Fig. 9. Attached to vertebra.

Three tests were carried out at increasing loads of 500, 750 (nominally 50% of ultimate failure load) & 950N; strain data was collected using LabView (National Instruments). Maximum values were measured for each gauge element, these raw values were then corrected for transverse sensitivity (Vishay technical note TN509) using the formulae in Figure 1.

$$\varepsilon_1 = \frac{\hat{\varepsilon}_1(1 - \nu_0 K_{t_1}) - K_{t_1} \hat{\varepsilon}_3(1 - \nu_0 K_{t_3})}{1 - K_{t_1} K_{t_3}}$$

$$\varepsilon_2 = \frac{\hat{\varepsilon}_2(1 - \nu_0 K_{t_2})}{1 - K_{t_2}} - \frac{K_{t_2} [\hat{\varepsilon}_1(1 - \nu_0 K_{t_1})(1 - K_{t_3}) + \hat{\varepsilon}_3(1 - \nu_0 K_{t_3})(1 - K_{t_1})]}{(1 - K_{t_1} K_{t_3})(1 - K_{t_2})}$$

$$\varepsilon_3 = \frac{\hat{\varepsilon}_3(1 - \nu_0 K_{t_3}) - K_{t_3} \hat{\varepsilon}_1(1 - \nu_0 K_{t_1})}{1 - K_{t_1} K_{t_3}}$$

Figure 1 - Transverse sensitivity formulae (Vishay TN509)

The corrected strain values were then used in **Error! Reference source not found.** and **Error! Reference source not found.** to calculate the principal strains ε_1 and ε_2 , and the angle of principal strain from the axis of the 'A' gauge.

$$\varepsilon_1 = \frac{1}{2} \cdot (\varepsilon_a + \varepsilon_c) + \frac{1}{2} \cdot \sqrt{(\varepsilon_a - \varepsilon_c)^2 + (2 \cdot \varepsilon_b - \varepsilon_a - \varepsilon_c)^2}$$

$$\varepsilon_2 = \frac{1}{2} \cdot (\varepsilon_a + \varepsilon_c) - \frac{1}{2} \cdot \sqrt{(\varepsilon_a - \varepsilon_c)^2 + (2 \cdot \varepsilon_b - \varepsilon_a - \varepsilon_c)^2} \quad (3)$$

$$\tan 2\phi = \frac{2 \cdot \varepsilon_b - \varepsilon_a - \varepsilon_c}{\varepsilon_a - \varepsilon_c} \quad (4)$$

3.3 Results

The FE model showed good agreement in terms of principal strain direction, however due to the limitations of the model in representing both the elastic modulus and bone anisotropy, the magnitude of principal strain showed a percentage error of 8% to 48% for spine 3, and 104% to 199% for spine 18 (**Error! Reference source not found.**), further work is required using a larger sample set to better quantify the principal strains and standard deviation before a conclusion can be presented.

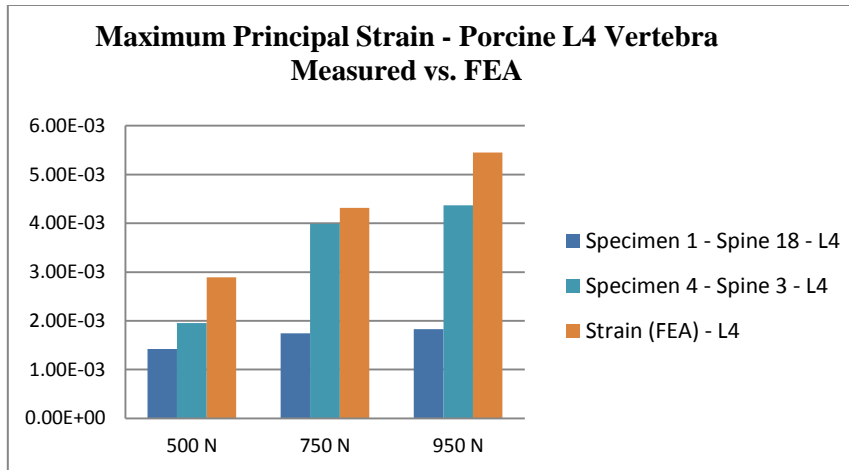


Fig. 11. Strain results (pilot study).

Acknowledgements

Funded by: Irish Research Council.

References

- B.M. Cyron, W.C. Hutton, J. D. . T. (1976). Spondylolytic Fractures. *The Journal of Bone and Joint Surgery*, 58-B(4), 462.
- Bisschop, A., Mullender, M. G., & Kingma, I. (2012). The impact of bone mineral density and disc degeneration on shear strength and stiffness of the lumbar spine following laminectomy, 530–536. doi:10.1007/s00586-011-1968-2
- Busscher, I., van der Veen, A. J., van Dieën, J. H., Kingma, I., Verkerke, G. J., & Veldhuizen, A. G. (2010). In vitro biomechanical characteristics of the spine: a comparison between human and porcine spinal segments. *Spine*, 35(2), E35–42. doi:10.1097/BRS.0b013e3181b21885
- Carter, D. R. (1977). The compressive behavior of bone as a two-phase porous structure. *The Journal of Bone and Joint Surgery*, 59(7), 954.
- Cendre, E., Mitton, D., Roux, J. P., Arlot, M. E., Duboeuf, F., Burt-Pichat, B., & Meunier, P. J. (1999). High-resolution computed tomography for architectural characterization of human lumbar cancellous bone: relationships with histomorphometry and biomechanics. *Osteoporosis International*, 10(5), 353–360.
- Crewe, H. (2013). Lumbo-pelvic loading during fast bowling in adolescent cricketers: The influence of bowling speed and technique. *Journal of Sports Sciences*.
- Dath, R., Ebinesan, a D., Porter, K. M., & Miles, a W. (2007). Anatomical measurements of porcine lumbar vertebrae. *Clinical Biomechanics (Bristol, Avon)*, 22(5), 607–13. doi:10.1016/j.clinbiomech.2007.01.014
- Dickey, J. P., Dumas, G. A., Bednar, D. A., & Sciences, N. (2003). Comparison of porcine and human lumbar spine flexion mechanics *, 44–49.
- Frymoyer, J. W. (1988). Back pain and sciatica. *The New England Journal of Medicine*, 318(5), 291.
- HensingerRN. (1989). Spondylolysis and spondylolisthesis in children and adolescents. *Journal of Bone and Joint Surgery*, 71(7), 1098–1107.
- Hobatho et al. (1997). *Bone Research in Biomechanics. Hobatho et al, 1997, Bone Research in Biomechanics*.
- Howarth, S. J., & Callaghan, J. P. (2013). Towards establishing an occupational threshold for cumulative shear force in the vertebral joint - An in vitro evaluation of a risk factor for spondylolytic fractures using porcine specimens. *Clinical Biomechanics (Bristol, Avon)*, 1–9. doi:10.1016/j.clinbiomech.2013.01.003
- Huiskes, R. (1983). A survey of finite element analysis in orthopedic biomechanics: The first decade. *Journal of Biomechanics*, 16(6), 385–409.

- Keaveny, T. M., & Yeh, O. C. (2002). Architecture and trabecular bone - toward an improved understanding of the biomechanical effects of age, sex and osteoporosis. *Journal of Musculoskeletal & Neuronal Interactions*, 2(3), 205–8. Retrieved from <http://www.ncbi.nlm.nih.gov/pubmed/15758434>
- Kettler, a, Liakos, L., Haegele, B., & Wilke, H.-J. (2007). Are the spines of calf, pig and sheep suitable models for pre-clinical implant tests? *European Spine Journal : Official Publication of the European Spine Society, the European Spinal Deformity Society, and the European Section of the Cervical Spine Research Society*, 16(12), 2186–92. doi:10.1007/s00586-007-0485-9
- Kuo, Y., & Wang, J. (2007). STRAIN ANALYSIS OF PARS INTERARTICULARIS AND ITS IMPLICATIONS IN THE SPONDYLOLYSIS, 19(2), 79–84.
- Lennon, A. B., & Prendergast, P. J. (n.d.). *Finite Element Modelling in Biomechanics and Mechanobiology*.
- Lin, R.-M. (1997). Distribution trabecular and regional strength of bone in the porcine lumbar Proximal. *Clinical Biomechanics*, 12(5), 1997.
- Michael Parfitt. A. (1987). Bone Histomorphometry: Standardization of Nomenclature, Symbols, and Units. *Journal of Bone and Mineral Research : The Official Journal of the American Society for Bone and Mineral Research*, 2(6).
- Muller, R., & Ruegsegger, P. (1997). Micro-tomographic imaging for the nondestructive evaluation of trabecular bone architecture. In *Bone Research in Biomechanics*.
- Nalla, R. K., Stölken, J. S., Kinney, J. H., & Ritchie, R. O. (2005). Fracture in human cortical bone: local fracture criteria and toughening mechanisms. *Journal of Biomechanics*, 38(7), 1517–25. doi:10.1016/j.jbiomech.2004.07.010
- Prendergast, P. J. (1997). Review Paper Finite element models in tissue mechanics and orthopaedic implant design. *Clinical Biomechanics*, 12(6), 343–366.
- Rho, J. Y., Hobatho, M. C., & Ashman, R. B. (1995). Relations of mechanical properties to density and CT numbers in human bone. *Medical Engineering & Physics*, 17(5), 347–355.
- Schmidt, R., Richter, M., Claes, L., Puhl, W., & Wilke, H.-J. (2005). Limitations of the cervical porcine spine in evaluating spinal implants in comparison with human cervical spinal segments: a biomechanical in vitro comparison of porcine and human cervical spine specimens with different instrumentation techniques. *Spine*, 30(11), 1275–82.
- Singer, K. (1995). Prediction of thoracic and lumbar vertebral body compressive strength: correlations with bone mineral density and vertebral region. *Bone*, 17(2), 167.
- Smit, T. H. (2002). The use of a quadruped as an in vivo model for the study of the spine - biomechanical considerations. *European Spine Journal : Official Publication of the European Spine Society, the European Spinal Deformity Society, and the European Section of the Cervical Spine Research Society*, 11(2), 137–144. doi:10.1007/s005860100346
- Tanck, E., Homminga, J., van Lenthe, G. H., & Huiskes, R. (2001). Increase in bone volume fraction precedes architectural adaptation in growing bone. *Bone*, 28(6), 650–4. Retrieved from <http://www.ncbi.nlm.nih.gov/pubmed/11425654>
- Taylor, D., Mulcahy, L., Presbitero, G., Tisbo, P., Dooley, C., & Lee, T. C. (2010). The Scissors Model of Microcrack Detection in Bone: Work in Progress, 1274.
- Taylor, D., O'Brien, F. J., & Lee, T. (2002). A theoretical model for the simulation of microdamage , repair and adaptation in compact. *Meccanica*, 37(4-5), 397–406.
- Teo, J. C. M., Si-Hoe, K. M., Keh, J. E. L., & Teoh, S. H. (2006). Relationship between CT intensity, micro-architecture and mechanical properties of porcine vertebral cancellous bone. *Clinical Biomechanics (Bristol, Avon)*, 21(3), 235–44. doi:10.1016/j.clinbiomech.2005.11.001
- Teoh, S. H., & Chui, C. K. (2008). Bone material properties and fracture analysis: needle insertion for spinal surgery. *Journal of the Mechanical Behavior of Biomedical Materials*, 1(2), 115–39. doi:10.1016/j.jmbbm.2007.06.004
- Van Lenthe, G. H., Van Den Bergh, J. P. W., Hermus, A. R. M. M., & Huiskes, R. (2001). The Prospects of Estimating Trabecular Bone Tissue Properties from the Combination of Ultrasound, Dual-Energy

- X-Ray Absorptiometry, Microcomputed Tomography, and Microfinite Element Analysis. *Journal of Bone and Mineral Research*, 16(3), 550–555.
- Wilcox, R. K. (2007). The influence of material property and morphological parameters on specimen-specific finite element models of porcine vertebral bodies. *Journal of Biomechanics*, 40(3), 669–73. doi:10.1016/j.jbiomech.2006.02.005
- Wilke, H.-J., Geppert, J., & Kienle, A. (2011). Biomechanical in vitro evaluation of the complete porcine spine in comparison with data of the human spine. *European Spine Journal : Official Publication of the European Spine Society, the European Spinal Deformity Society, and the European Section of the Cervical Spine Research Society*, 1859–1868. doi:10.1007/s00586-011-1822-6
- Wiltse, L. L. (1957). Etiology of spondylolisthesis. *Clinical Orthopaedics*, 10, 48.